International Journal of Rock Mechanics and Mining Sciences 110 (2018) 111–119

Contents lists available at ScienceDirect

International Journal of Rock Mechanics and Mining Sciences

journal homepage: www.elsevier.com/locate/ijrmms

Experimental investigation on fracture propagation modes in supercritical carbon dioxide fracturing using acoustic emission monitoring

Dawei Zhou, Guangqing Zhang*, Yuanyuan Wang, Yuekun Xing

College of Petroleum Engineering, China University of Petroleum-Beijing, Beijing 102249, China

ARTICLE INFO

Keywords:
Supercritical CO_2 fracturing
AE signals analysis
Fracture network
Fracture propagation modes

ABSTRACT

Supercritical carbon dioxide (SC-CO_2) fracturing has broad application prospects due to its potential to increase production, to reduce water requirements, and to minimize environmental impacts. To date, lowering fracture breakdown pressure and inducing multi-fractures using SC-CO_2 as fracturing fluid have been recognized, but the process of fracture propagation has been poorly studied. Therefore, acoustic emission (AE) system with 12 channels is used to monitor the SC-CO_2 fracturing. The results show that energy release rate of SC-CO_2 fracturing is 1–3 orders of magnitude higher and the cumulative energy is also much larger compared to hydraulic fracturing. Then much available energy can be converted into driving force to generate dynamic multi-fractures. Meanwhile, the curves of cumulative energy are observed as shape of sidestep or zigzag. The SC-CO_2 fracturing evolution of AE events is discontinuous, suggesting that intermittent fracture propagation occurs. The process and modes of SC-CO_2 fracture propagation are proposed, respectively. The process of SC-CO_2 fracture propagation can be divided into 4 stages: damage zone evolution, fracture initiation, fracture post-instability and fracture arrest. And fracture propagation modes are classified into 3 types, including single curved fracture (Type -I), fracture band (Type -II) and fracture network (Type -III). This study is helpful for designing appropriate treatment to optimize CO_2 sequestration or to enhance stimulated reservoir volume.

1. Introduction

Numerous techniques and methods such as injection pressure decline analysis, microseismic monitoring technique, tiltmeter fracture mapping technology, radioactive tracer monitoring and others, are available to diagnose fracturing performance in the field. However, fracture propagating process and fracture morphology are not directly observed using those methods mentioned above. Similarly, numerical models are built to simulate fracture propagation based on over-simplified conditions, resulting in a discrepancy with the field-scale application.

It is a ubiquitous phenomenon that acoustic emission (AE) signals are produced by rapid microcrack growth associated with brittle fracture.[1] AE parameter and AE localization analyses are widely used to investigate rock failure process under compressive stress.[2] According to literature reviews related to hydraulic fracturing monitoring, the involved experimental methods are as follows: observational method,[3–5] active ultrasound monitoring,[6,7] AE monitoring[8–10] and fiber optic measurement technology.[11–13] Due to restrictions of testing device and specimen size, computed tomography (CT) and scanning electron microscope (SEM) failed to monitor hydraulic fracturing process up to now.[14] So the mechanism of hydraulic fracture propagation is usually studied using AE monitoring indoors. Analysis of AE signals and optical microstructures indicates a process of three stages characterized with elastic deformation, nucleation and propagation of breakouts in borehole breakout evolution.[9] Both AE event frequency and focal mechanisms (FMS) illustrate that shear failure is more common than tensile failure, and sequential AE activity is found to be episodic and discretized, implying fracture propagation is not simply continuous in hydraulic fracturing.[10]

Currently, experimental results show that AE signals distribute more widely by SC-CO_2 or L-CO_2 fracturing than by hydraulic fracturing, because fracturing fluid of low viscosity tends to generate extensive micro-fractures.[8,15–17] Correspondingly, some field tests indicate that many more microseismic signals are recorded in SC-CO_2 fracturing compared with in hydraulic fracturing.[18,19] Energy levels and frequency of AE signals share similar patterns between SC-CO_2 and hydraulic fracturing, showing that much of the abundant experience relating to hydraulic fracturing can be applied to CO_2 fracturing.[19] As an emerging reservoir stimulation treatment, SC-CO_2 fracturing is little studied with

* Correspondence to: College of Petroleum Engineering, China University of Petroleum-Beijing, Room 802, North Wing, ZhongYou Building, Beijing 102249, PR China.

E-mail address: zhangguangqing@cup.edu.cn (G. Zhang).

https://doi.org/10.1016/j.ijrmms.2018.07.010
Received 28 November 2017; Received in revised form 29 June 2018; Accepted 28 July 2018

respect to fracture propagation modes. It is usually based on the previous hydraulic fracture models to perform numerical stimulation or to optimize CO_2 fracturing treatments in the field. But physical and chemical properties of CO_2 vary with the temperature and pressure, making it a unique treatment fluid.[20,21] And significant differences may occur in dynamic behavior depending on whether the fracturing fluid is water or CO_2. Therefore, to distinguish the fracture behaviors between SC-CO_2 and hydraulic fracturing, AE monitoring is used to study the process and modes of SC-CO_2 fracture propagation in this paper.

2. Experimental procedures of SC-CO_2 fracturing

2.1. Specimen preparation

Laboratory tests were conducted on manufactured cubic specimens (30 cm × 30 cm × 30 cm) which was made with composite Portland cement of PC32.5 R and quartz sand of 40–70 mesh. Cement and quartz sand were mixed by mass ratio 1:1 and specimens were maintained for 2 weeks. The mechanical properties of the specimen were obtained by compressive and tensile experiments, with uniaxial compressive strength of 27.89 MPa, tensile strength of 3.55 MPa, Poisson's ratio of 0.17 and elastic modulus of 24.6 GPa.

To position the AE signals, 12 AE sensors were placed on 4 faces of the specimen (Fig. 1(a)) covered with vaseline to alleviate the noise induced by friction between hydraulic ram and specimen surface during loading (Fig. 1(b)). The threshold value of AE amplitude analysis system was 40 dB and sampling frequency was 10 MHz.

2.2. Testing procedure

Experiments were performed using the 200R3-CO_2 system.[22] To simulate SC-CO_2 fracturing, CO_2 firstly released from a CO_2 container was injected into cooling tank ($T < 2$ ℃) to change into liquid state completely. Then the liquid CO_2 was pressurized by injection pump and subsequently heated by heating tank to reach supercritical state ($T > 31$ ℃, $P > 7.38$ MPa). In this way, CO_2 can be transformed into SC-CO_2 before being injected into the specimen. Before testing, the specimen was placed in heating box with sustained temperature of 45 ℃ for four hours. During testing, the temperature of fracturing apparatus was also maintained at 45 ℃ until ending the testing in order to reach supercritical temperature.

Two types of fracturing fluids, i.e., water-based fracturing fluid mixed with guar gum and SC-CO_2, were used. For possible application in the field, we used guar gum to increase the viscosity of fracturing fluid to 106 cP. Various horizontal stress differences and injection rates were considered (Table 1). After testing, both fracture morphology and AE signal characteristic were analyzed to investigate SC-CO_2 fracture behaviors.

Table 1
Testing program for hydraulic and SC-CO_2 fracturing.

Specimen No.	Fracturing fluid	$\sigma_v - \sigma_H - \sigma_h$ (MPa)	Injection rate (mL/min)
1-1#	Water + guar gum	23-21-19	2
2-1#	SC-CO_2	23-21-19	26
2-2#		23-21-17	
2–3#		23-21-15	
2–4#		23-21-13	
2–5#		23-21-11	

3. Fracture morphology and propagation analysis

3.1. Fracture morphology in macroscopic and microscopic aspects

Fracture morphology analysis seems to be the most direct and simple method for evaluation of hydraulic fracture performance.[23] In order to observe fracture paths directly, we cut the specimen in the middle cross-section perpendicular to the maximum principal stress. It can be seen that hydraulic fracture paths are simply curved fractures, however, SC-CO_2 fracture paths are more complex (Fig. 2). We will study the fracture characteristics from macroscopic and microscopic aspects, respectively.

To describe macroscopic fractures, we firstly define a fracture band as a group of secondary or branching fractures near the main fractures. For small stress difference ($\Delta\sigma$<6MP), fracture networks and fracture bands are generated in SC-CO_2 fracturing (Fig. 2(b)-(d)). For larger stress difference, the number of macro-fractures reduces and fracture paths deflect (Fig. 2(e), (f)), similar to that of hydraulic fracturing (Fig. 2(a)). Therefore, when stress difference is less than 6MP a, it has a little influence on SC-CO_2 fracture growth and morphology, provided that pore pressure is larger than the CO_2 critical pressure of 7.38 MPa. Fracture networks and fracture bands are more likely to be induced (Fig. 2(b)-(d)). Besides the reservoir rock property, in-situ stress and pore pressure, both fluid rheology and leakoff properties are also key parameters to determine the fracture behaviors driven by fluid.[24] Due to CO_2 properties largely depend on pressure and temperature, SC-CO_2 fracture behaviors are less affected by the stress difference when it is less than 6 MPa.

To illustrate fracture complexity, we use the concept of fracture tortuosity defined as the ratio of total fracture length to the direct length of two ends in the reference area.[16] As an essential parameter to determine the stimulated reservoir volume in hydraulic fracturing, the fracture tortuosity also seems useful in evaluating its impacts on fluid flow in fractures.[25] We calculate fracture tortuosity of 6 specimens by digitizing macro-fracture paths on the middle cross-section with a sampling interval of 1 mm, which shows that fracture tortuosity

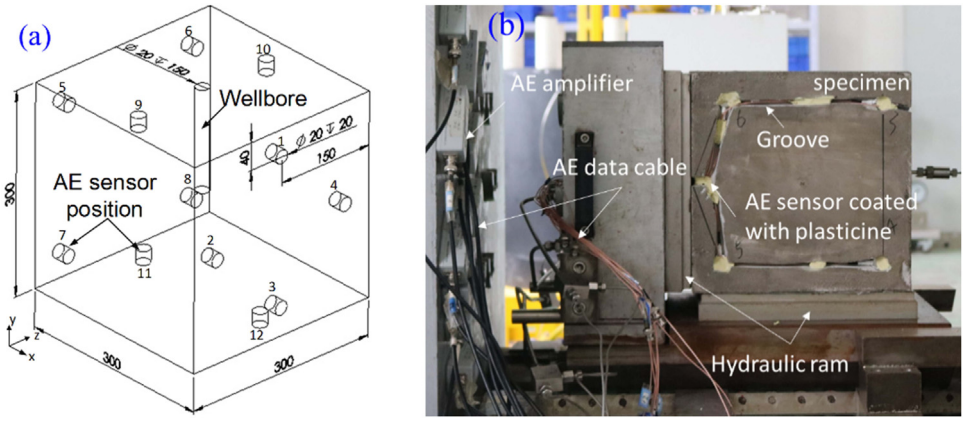

Fig. 1. (a) Sketch of AE sensor layout (Unit: mm) and (b) specimen in testing.